

See discussions, stats, and author profiles for this publication at: <https://www.researchgate.net/publication/259586143>

Preliminary Hazard Evaluation of Androgen Receptor-Mediated Endocrine-Disrupting Effects of Thioxanthone Metabolites through Structure-Based Molecular Docking

ARTICLE in CHEMICAL RESEARCH IN TOXICOLOGY · JANUARY 2014

Impact Factor: 3.53 · DOI: 10.1021/tx400383p · Source: PubMed

CITATIONS

2

READS

42

3 AUTHORS:



Tiziana Ginex

Università degli studi di Parma

7 PUBLICATIONS 4 CITATIONS

SEE PROFILE



Chiara Dall'Asta

Università degli studi di Parma

131 PUBLICATIONS 1,877 CITATIONS

SEE PROFILE



Pietro Cozzini

Università degli studi di Parma

98 PUBLICATIONS 1,657 CITATIONS

SEE PROFILE

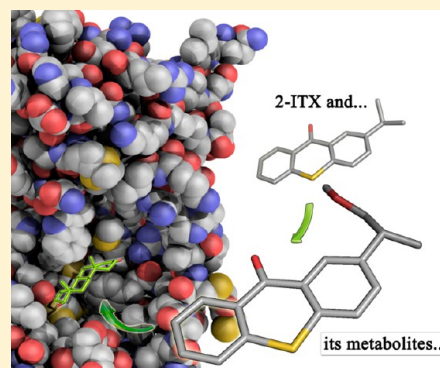
Preliminary Hazard Evaluation of Androgen Receptor-Mediated Endocrine-Disrupting Effects of Thioxanthone Metabolites through Structure-Based Molecular Docking

Tiziana Ginex,[†] Chiara Dall'Asta,[‡] and Pietro Cozzini^{*,†}

[†]Molecular Modelling Laboratory, Department of Food Science, University of Parma, Parco Area delle Scienze, 17/A, 43124 Parma, Italy

[‡]Department of Food Science, University of Parma, Parco Area delle Scienze, 59/A, 43124 Parma, Italy

ABSTRACT: Foodstuff could be a vector for naturally occurring and/or unwanted dangerous substances that can act either as they are or after their bioactivation. The scientific community agrees that the metabolic activity of chemicals should be taken into account for proper risk assessment. Unfortunately, the *in vitro* evaluation of a metabolic panel and analytical/biochemical detection in food-safety assessment are very expensive and challenging because of the abundance of data to analyze. In this context, properly validated computational protocols could be a useful tool for making metabolic and binding/activity predictions. This strategy has been applied to thioxanthone photoinitiators (TX), identified as food contaminants, especially in infant formulas, as reported by the European Food Safety Authority in 2005. Their lipophilicity suggests rapid hepatic metabolism, but the currently available data only concern 2-ITX. We have predicted phase I metabolites for the TX class of compounds and defined their binding affinity for the AR ligand-binding pocket using a local model based on available information about metabolism and AR activity. Some metabolites should undergo further *in vitro* or/and *in vivo* toxicological evaluations because they have proved to be suitable as ligands for AR.



INTRODUCTION

To function correctly, the human body needs functional nutrients retrieved from a wide variety of foods. However, foodstuff could be a vector for naturally occurring and/or unwanted dangerous substances that can act either as they are or after their bioactivation. The scientific community agrees that the metabolic activity of chemicals should be taken into account for proper risk assessment. Unfortunately, the *in vitro* evaluation of a metabolic panel and analytical/biochemical detection in food-safety assessment are very expensive and challenging because of the abundance of data to analyze. Moreover, the scientific community needs new technologies for a faster, cheaper, easier, and more accurate evaluation of metabolites and their parents. In this context, *in silico* technologies could provide a valid support for metabolic and binding/activity predictions. If properly validated, such approaches could allow the detection, quantification, and toxicological evaluation to be focused only on those metabolites previously identified as being potentially toxic, in accordance with EFSA policies. The traditional approach and new perspectives offered by *in silico* techniques are summarized in Scheme 1.

Here, we report a case study of the structure–toxicity relationship for thioxanthone photoinitiators. Thioxanthenes are widely used in food packaging. They are added in pigmented formulations as photoinitiator/sensitizers during UV-curing ink-polymerization procedures. Because of their long triplet

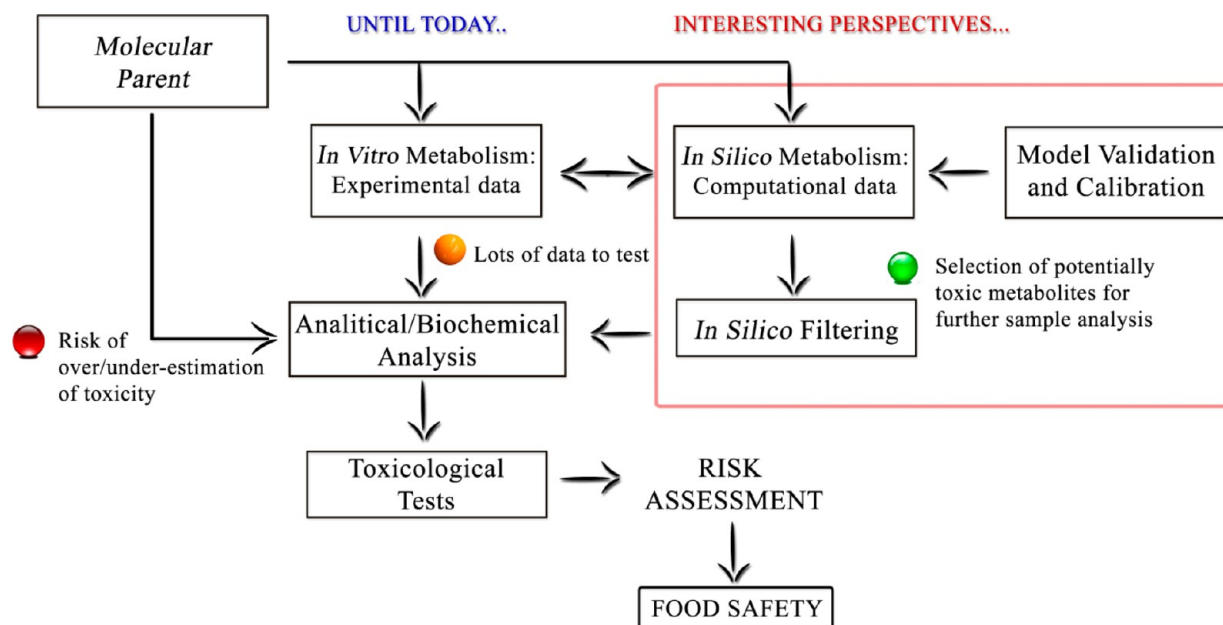
lifetimes, which can lead to quenching reactions, thioxanthone (TX) compounds promote efficient and rapid ink polymerization even at low temperatures, which preserves the lifetime of UV-LED lamps. Despite their good chemical properties, some cases of food contamination have occurred. In 2005, the European Food Safety Authority (EFSA) reported the results of analytical tests on the levels of ITX and EHDAB in a number of food products packaged in cartons printed with UV-cured inks containing isopropyl thioxanthone (ITX) and 2-ethylhexyl-4-dimethylaminobenzoate (EHDAB) as photoinitiators.¹ In infant formulas, ITX has been found at levels ranging from 120 to 305 $\mu\text{g/L}$, whereas in milk- and soy-based foods not specifically intended for babies, ITX reached levels ranging from 54 to 219 $\mu\text{g/L}$. The panel noted that infants exclusively fed with infant formulas packed in cartons printed with UV-cured inks are potentially exposed to more ITX and EHDAB than other population groups because of their high consumption of food per kilogram of body weight.

From a toxicological point of view, Peijnenburg, Reisma, and respective co-workers^{2,3} (personal communication) previously analyzed AhR-agonistic, -antiandrogenic, and -antiestrogenic effects of some TX compounds using a dioxin receptor chemical-activated luciferase gene-expression assay (DR CALUX) and yeast-based androgen and estrogen bioassays,

Received: October 11, 2013

Published: January 6, 2014



Scheme 1. Schematic Representation of Traditional Safety Assessment and Implementation with *in Silico* Techniques

respectively. The chemical structures of 2- and 4-ITX, 2,4-diethyl-TX, 2-chloro-TX, and 1-chloro-4-propoxy-TX are reported in Figure 1. When tested alone, none of these five

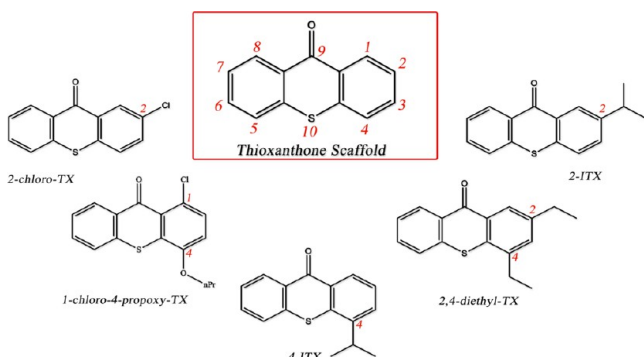


Figure 1. Chemical structures of the five synthetic tioxanthenes analyzed by Reitsma and co-workers.³

compounds have shown agonistic activity. With the exception of 1-chloro-4-propoxy-TX, all tested compounds have been capable of displacing the endogenous ligand, testosterone, in concentrations of 0.07 and 1 μ M, thus showing antiandrogenic behavior with no cytotoxic effects.

The androgen receptor (AR) is a 3-ketosteroid receptor and belongs to a large family of ligand-inducible transcriptional factors identified as nuclear receptors.⁴ AR has four main structural and functional domains. Among them, the AR ligand-binding pocket (LBP) is located in the C-terminal domain (CTD). The binding of the endobiotic ligand testosterone or its more potent 5 α -reductase-derived metabolite DHT to the LBP induces protein homodimerization and translocation into the nucleus, where the recruitment of cofactor proteins and the activation of transcriptional machinery takes place.^{5,6}

From a metabolic point of view, Aprile and co-workers⁷ (personal communication) investigated the metabolic stability of 2-ITX in human and liver subcellular fractions *in vitro* by incubating the chemical with rat liver microsomes (RLM) and

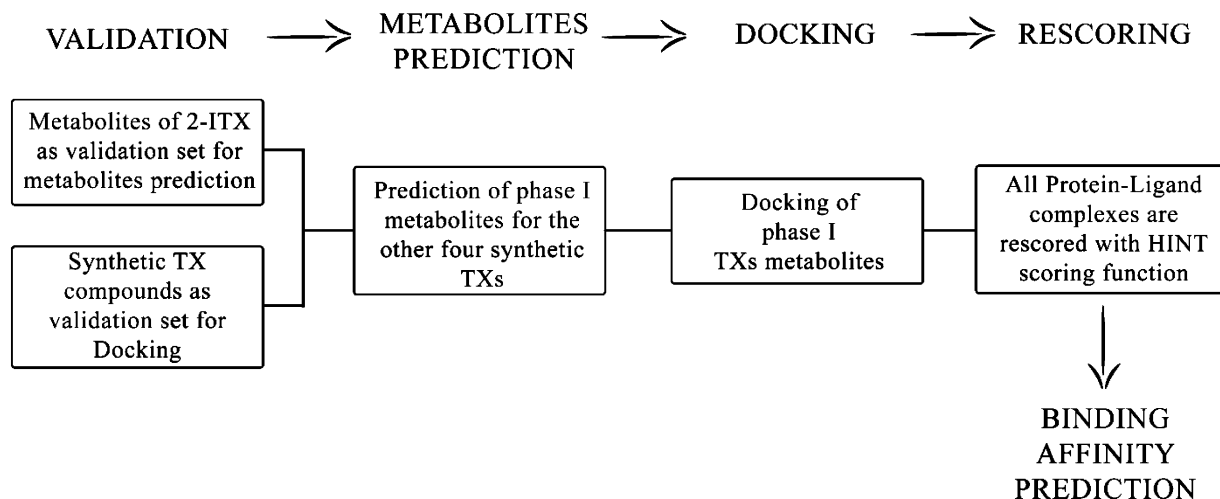
human liver microsomes (HLM). After reaction and purification steps, each sample was injected into an LC/MS column for analysis. The structures of eight metabolites were defined by comparing their mass spectra with those of synthetic reference compounds. When 2-ITX was incubated in the presence of RLM, the formation of the 2-(1,2-diol) derivative was observed; the oxidation of the 2-(propen-2-yl) derivative could lead to the generation of an epoxide intermediate, which is completely hydrolyzed by epoxide hydrolases. High TX lipophilicity implies rapid human hepatic metabolism, but this does not always result in detoxification. Currently, despite the androgen-disrupting effects of the five synthetic TX compounds and the metabolic pathway of 2-ITX, no further metabolic/toxicological considerations are available.

Previously reported data on 2-ITX metabolism and AR activity was used as a validation set for making metabolic and binding-affinity predictions, respectively. In this way, a computational approach was performed to predict putative metabolites and to define the potential AR-related endocrine-disrupting effects of the TX class of compounds. Our final results suggest that further *in vitro* studies could be necessary for a more concrete risk assessment.

MATERIALS AND METHODS

Protein and Chemicals. For the receptor, the crystal structure of the agonist-bound androgen receptor in complex with its endogenous ligand, testosterone,⁸ was used in these studies (PDB: 2AM9, resolution (\AA), 1.64; mean B value, 27.38; pH 7.6. 2AM9 was selected because of its good crystallographic properties in terms of resolution, protonation states (pH), and B-factor (index of structural stability), which are crucial to have for a starting material to be suitable for *in silico* analysis. Moreover, 2AM9 was able to reproduce correctly experimental data on the AR activity of TX compounds. Among the 52 available crystallographic structures of AR, there is no structural model of WT antagonism. We tried to model AR competitive antagonism starting from a crystallographic structure of 2AM9; the assumption is that compounds with an affinity greater than that of the natural ligand for the AR-LBP could be able to displace it in a competitive manner, influencing physiological AR activity. Hydrogen atoms were added in Sybyl v.8.1 (Tripos, Inc., St. Louis, MO) and were energy-minimized

Scheme 2. Schematic Representation of Computational Protocol



using the Powell algorithm with a convergence gradient of 0.5 kcal (mol Å)⁻¹ for 1500 iterations. All water molecules, other solvents, and the crystallographic ligand were deleted.

For chemicals, 2-ITX, 4-ITX, chlorinated (2-chloro-TX), alkyl derivative (2,4-diethyl-TX), 1-chloro-4-propoxy-TX, (R)- and (S)-2-(1-hydroxypropan-2-yl)-TX (R-M1; S-M2), 2-(2-hydroxypropan-2-yl)-TX (M3), 2-(prop-1-en-2-yl)-TX (M4), (R)- and (S)-2-(2-methyloxiran-2-yl)-TX (R-M5; S-M6), 2-(2-hydroxypropan-2-yl)-TX-10-oxide (M7), 2-isopropyl-TX-10-oxide (M8), (R)- and (S)-2-(1,2-dihydroxypropan-2-yl)-TX (R-M9; S-M10), 1-chloro-4-hydroxy-TX (M11), 1-chloro-6-hydroxy-4-propoxy-TX (M12), 1-chloro-4-propoxy-TX 10-oxide (M13), 2,4-diethyl-TX-10-oxide (M14), 2-chloro-TX-10-oxide (M15), 2-chloro-6-hydroxy-TX (M16), 6-hydroxy-2-isopropyl-TX (M17), 4-(2-hydroxypropan-2-yl)-TX (M18), 4-isopropyl-TX-10-oxide (M19), 2,4-diethyl-6-hydroxy-TX (M20), 6-hydroxy-4-isopropyl-TX (M21), 2-ethyl-4-((R)-1-hydroxyethyl)-TX (M22), and 2-ethyl-4-((S)-1-hydroxyethyl)-TX (M23) were built in Sybyl and then energy-minimized with a convergence gradient of 0.05 kcal (mol Å)⁻¹ for 100 iterations.

All structures (protein and chemicals) were checked for the correct assignment of atom and bond type and then saved as .mol2 files.

Computational Protocol. The entire protocol is summarized in Scheme 2. Briefly, it consists of validation, metabolites prediction, docking, rescoring, and binding-affinity prediction. A validation step was performed to test the suitability of our approach in metabolite and binding predictions. Metabolites identified by Aprile and co-workers for 2-ITX (M1–M10) were used to test the performance of MetaPrint2D in site of metabolism (SOM) predictions, whereas the five TX compounds of Reitsma and co-workers were used as a validation set for docking predictions.

Validation of MetaPrint2D Predictive Performance. MetaPrint2D phase I predictions for the thioxanthone scaffold, which are based on a P450's general model, are reported in Figure 2; the C2-isopropyl moiety, S10, and C6 were identified as the sites of the molecular scaffold that are the most likely to undergo phase I metabolism. Aliphatic C-hydroxylation, desaturation, and sulfoxidation as well as aromatic C-hydroxylation are the most likely mechanisms. The NOR value in rat and human models of metabolism (R-NOR and H-NOR, respectively) were calculated to reproduce the same experimental conditions virtually. In the case of the TX scaffold, the model was able to predict oxidative metabolism correctly. Moreover, the *in silico* predictions agree with the experimental results that suggest a particular metabolic regioselectivity that is mainly focused on the isopropyl moiety and sulfur atom. Aliphatic C-hydroxylation of the 2-isopropyl moiety was correctly predicted (M1–M3, M9, and M10). Desaturation of the isopropyl moiety leads to the formation of olefin M4. M7 and M8 result from sulfoxidation in both human and rat models (NOR = 1.00). Computational predictions also suggest

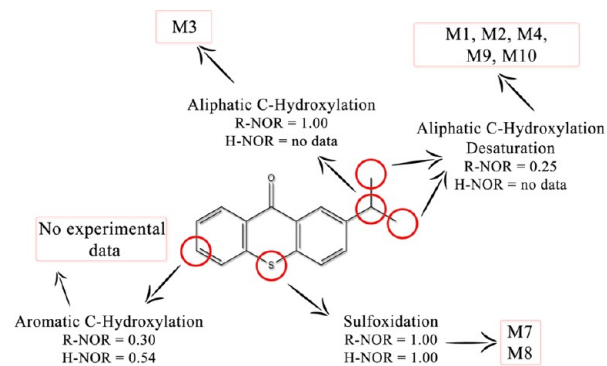
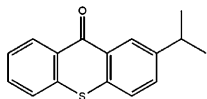
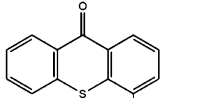
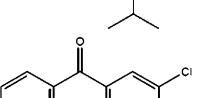
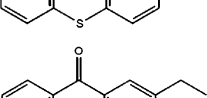
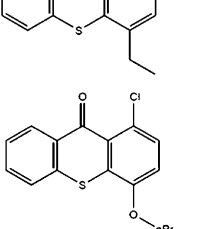


Figure 2. MetaPrint2D predictions for the thioxanthone scaffold. As shown, the isopropyl moiety, S10, and C6 were identified as the sites of the molecule that are most likely to undergo phase I metabolism. The NOR value in rat and human models of metabolism (R-NOR and H-NOR, respectively) were calculated to reproduce the same experimental conditions virtually. In the case of the TX compound, the model was able to predict oxidative metabolism correctly. No experimental data is provided for C₆ aromatic C-hydroxylation.

aromatic C-hydroxylation in C6, especially in the human model, but there was no experimental confirmation of this. Epoxide derivatives M5 and M6 are not predicted by MetaPrint2D-React. However, Aprile and co-workers proposed the formation of an unstable epoxide from the olefin moiety of M4, but they point out that it was not found in extracts because of its rapid hydrolysis to the corresponding 1,2-diol derivatives (M9 and M10).

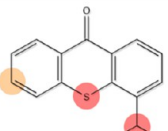
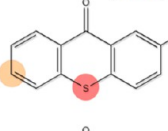
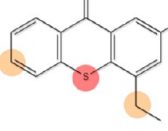
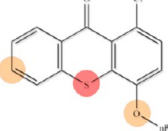
Validation of Docking Performance. A comparison between *in vitro* ligand-mediated transcriptional activity and *in silico* binding affinity for the validation set is reported in Table 1. Testosterone was considered as a reference compound (HS = 350). Binding affinity is expressed both in absolute (HS) and relative (affinity ratio) terms. Compounds with HS values greater than testosterone show a higher affinity for AR-LBP and might be able to compete with the endogenous ligand for AR-LBP binding. The affinity ratio expresses the index of the binding affinity relative to testosterone; in other words, it is the ratio between the HS of a tested compound and the HS of testosterone. 2-ITX, 4-ITX, and 2-chloro-TX show an affinity 2 to 3 times greater than testosterone; 2,4-diethyl-TX has an affinity ratio less than 1, and it is considered either to not or to be less capable of significantly competing with endogenous ligand testosterone. There are no likely poses for 1-chloro-4-propoxy-TX because of its bulky propoxy moiety. Docking results for tested compounds are in good agreement with available experimental data where the clear sigmoidal

Table 1. Androgen Receptor-Mediated Endocrine-Disrupting Effects of the Validation Set: Comparison between *in Vitro* Ligand-Mediated Transcriptional Activity and *in Silico* Binding Affinity for TX Chemicals

COMPOUND	STRUCTURE	<i>In vitro</i> ACTIVITY IC ₅₀ (μM) ^a	HS	AFFINITY RATIO (HS _{Comp} /HS _{Ref}) ^b
2-ITX ^c		1	1005	2.87
4-ITX ^c		1	1014	2.90
2-Chloro-TX ^c		2,5	888	2.54
2,4-Diethyl-TX ^c		9	306	0.87
1-Chloro-4-propoxy-TX ^c		-	No Likely Pose	-

^aExperimental activity has been reported as the concentration of a tested compound that induces a halving of the fluorescence signal in the presence of agonist testosterone.³ Androgen-mediated transcriptional activity has been tested on yeast hormone bioassays that express h-AR and green fluorescent reporter protein.^{9,10} Except for 1-chloro-4-propoxy-TX, all tested compounds from the reference set are capable of displacing endogenous ligand testosterone at concentrations of 0.07 and 1 μM. ^bReference compound, testosterone (HS = 350 pt). The affinity ratio is expressed as HS_{Comp}/HS_{ref}. The affinity ratio for testosterone is 1. ^cAlready tested *in vitro*.³

Table 2. MetaPrint2D Predictions: Hypothesized Mechanism, Metabolites, and Respective NOR Values for the Four Synthetic TX Compounds of the Validation Set

Compound	Structure	Hypothesized Mechanism	Predicted Metabolites	NOR value
4-ITX		S: Sulfoxidation	M19	1.00
		C6: Aromatic C-hydroxylation	M21	0.50
		C1': Aliphatic C-hydroxylation	M18	1.00
2-chloro-TX		S: Sulfoxidation	M15	1.00
		C6: Aromatic C-hydroxylation	M16	0.50
2,4-diethyl-TX		S: Sulfoxidation	M14	1.00
		C6: Aromatic C-hydroxylation	M20	0.50
		C3': Aliphatic C-hydroxylation	M22/M23	0.50
1-chloro-4-propoxy-TX		S: Sulfoxidation	M13	1.00
		C6: Aromatic C-hydroxylation	M12	0.50
		nPrO-C4: O-Dealkylation	M11	0.50

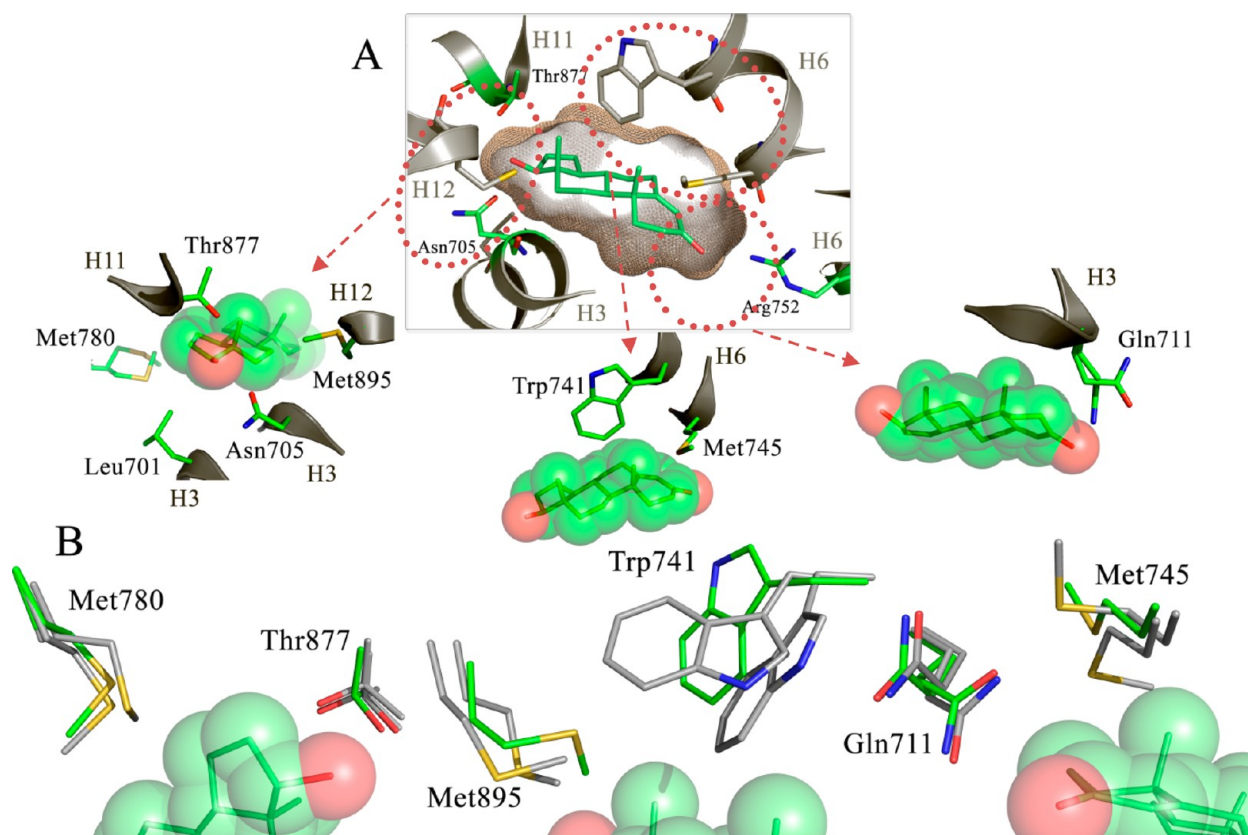


Figure 3. (A) Representation of AR-LBP (PDB ID: 2AM9). H-bond residues are highlighted as green sticks (Thr877, Asn705, and Arg752). The three red circles identify regions considered flexible during docking simulations: Leu701 (H3; C-terminal), Asn705 (H3; C-terminal), Met780 (H8; C-terminal), Thr877 (H11; C-terminal), and Met895 (H12; N-terminal) are in front of 17 β -OH moiety and Trp741 (H6; N-terminal) and Met745 (H6) are over the steroid scaffold, whereas Gln711 (H3) is placed in front of the 3-keto carbonyl of testosterone. The cavity shape is shown as a wheat wireframe. (B) Superposition of AR-LBP for 2AM9 (full-agonist testosterone), 3RLJ (nonsteroidal modulator, SARM S22), and 2PNU (steroidal modulator, EM-5744); side-chain orientations for 2AM9 are reported in green, whereas side-chain orientations for 3RLJ and 2PNU are reported in gray.

response of testosterone is inhibited by TX compounds in the following order: 2-ITX, 4-ITX, 2-chloro-TX, and 2,4-diethyl-TX. No androgenic activity was registered for 1-chloro-4-propoxy-TX.

Metabolite Prediction. After validation, the web interface of MetaPrint2D-React was used to predict phase I metabolites for 4-ITX, 2-chloro-TX, 2,4-diethyl-TX, and 1-chloro-4-propoxy-TX; each chemical was uploaded as an isomeric SMILES string generated by ChemBioDraw Ultra 12.0. Reaction types, phase I metabolites, and respective NOR values for the four synthetic TX compounds are summarized in Table 2. Only chemicals with NOR values greater than 0.5, referring to more plausible metabolites, were taken into account for docking. In particular, oxidative metabolism on S10 (sulfoxidation) was predicted for all thioxanthenes (NOR = 1.00); in this way, **M13**, **M14**, **M15**, and **M19** were obtained. Aromatic C6-hydroxylation (NOR = 0.5) for all thioxanthenes leads to the formation of **M12**, **M16**, **M17**, **M20**, and **M21**. *In vitro* metabolic studies of 2-ITX, mainly focused on rat metabolism, have not shown the formation of C6-hydroxyl derivatives; however, C-hydroxylation for polyaromatic scaffolds is frequently reported in the scientific literature, as in the case of PCBs.^{11–13} For this reason, we decided to include these derivatives (**M12**, **M16**, **M17**, **M20**, and **M21**) in our study as well. Metabolic predictions for 2,4-diethyl-TX also suggest the formation of **M22** and **M23** as a result of aliphatic C-hydroxylation at the level of the C4-isopropyl moiety (NOR = 0.5). O-Dealkylation was also predicted for 1-chloro-4-propoxy-TX (**M11**; NOR = 0.5).

Docking and Rescoring. Each predicted chemical (**M11–M23**) was docked into AR-LBP. After docking, the GOLD output was energetically revalued and properly ranked with the use of the HINT algorithm and scoring function. Generally, a high HINT score is

associated with a good binding result (see the following section). A suitable positioning of each chemical into the binding site as well as the energetic ranking proposed by the HINT scoring function were taken into account for final considerations.

Software and Procedures. Sybyl v.8.1 was used for protein and chemical preparations.

MetaPrint2D-React was used as the metabolite and reaction-type predictor tool. The software predicts the sites of a molecule that are most likely to undergo phase I metabolism based on their similarity to known sites of metabolism and to sites that are known not to be metabolized. The method is based on a database of atom environments found in molecules known to undergo metabolic transformation, such as the data found in the Symyx(R) (previously MDL) metabolite database that has collected over 80 000 metabolic transformations of xenobiotics curated from reports in the scientific literature. This database contains information about phase I additions (C-hydroxylations and other oxidations), eliminations (dealkylations and amide/ester hydrolysis reactions), and phase II additions (conjugations, etc.).

For metabolic predictions, the atom environments of a query molecule are calculated, and the database is searched for similar environments. Then, an occurrence ratio is calculated for each atom in the molecule; this measures how often this or a similar environment has been found at a reaction center relative to how many times it has been observed in total. To have a standard output, these ratios are then scaled so that the molecule's most likely site of metabolism is given a normalized occurrence ratio (NOR) of 1.^{14,15} The derived NOR value is represented with a customizable color code that goes from white (NOR = 0) to red (NOR = 1). This method was capable of correctly

identifying the first three most likely sites of metabolism in 87% of the external validation molecule set with a confidence of 90% in an internal validation procedure. Figure 3 provides an example of MetaPrint2D-React metabolite prediction for 2-ITX.

A semiflexible docking was performed with GOLD suite v. 5.1 (CCDC, Cambridge, UK). AR .mol2 files and all chemicals were loaded into the GOLD docking program. A default radius of 10 Å, from the coordinates of the central atom of crystallographic ligand testosterone, was used to direct the site location into the AR binding cavity. In this way, a suitable coverage of the active site was reached. Ligand flexibility was added before computation. The number of genetic algorithm (GA) runs was set to a maximum of 50 poses for each molecular candidate. For the genetic algorithm run, a maximum number of 100 000 operations were performed on a population of 100 individuals with a selection pressure of 1.1. Operator weights for crossover, mutation, and migration were set to 95, 95, and 10, respectively. The number of islands was set to 5, and the niche size was set to 2. The default GOLDScore fitness function was applied for performing the energetic evaluations.^{16,17} The distance for hydrogen bonding was set to 2.5 Å, and the cutoff value for the van der Waals calculation was set to 4.0 Å. To define side-chain flexibility on AR, available crystals were subjected to geometrical superposition (alignment by secondary structure). All of the information collected on the stability/flexibility of some amino acid side chains (Leu701, Asn705, Gln711, Trp741, Met745, Met780, Thr877, and Met895) was used to perform a proper computational approach to reach accurate predictions. To provide a rapid explanation of a more accurate comparison process, we have selected the three most representative crystals. As shown in Figure 4, the superposition of AR cocrystallized

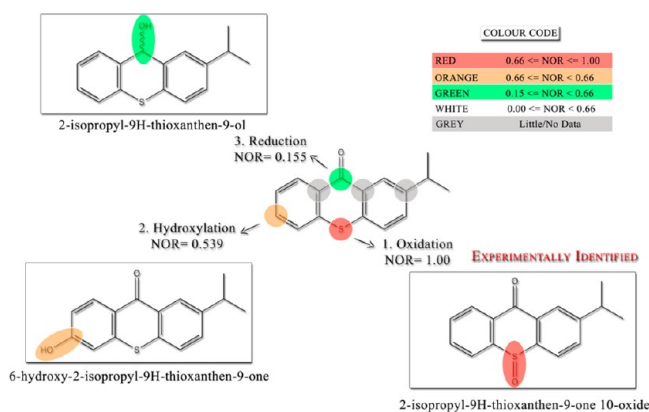


Figure 4. Example of MetaPrint2D-React molecular data mining. The predicted sites of metabolism (SOM) for 2-ITX are reported. As shown, the computationally proposed 2-isopropyl-TX-10-oxide (**M8**) was also experimentally identified. Only chemicals with NOR values greater than 0.5, referring to more plausible metabolites, were taken into account for *in silico* evaluations.

with a full agonist (PDB 2AM9), a nonsteroidal modulator¹⁸ (PDB 3RLJ), and a steroidal modulator¹⁹ (PDB 2PNU) revealed important ligand-induced crystallographic flexibility for Leu701, Asn705, Gln711, Trp741, Met745, Met780, Thr877, and Met895. Three main red-circled regions can be defined: Leu701 (H3; C-terminal), Asn705 (H3; C-terminal), Met780 (H8; C-terminal), Thr877 (H11; C-terminal), and Met895 (H12; N-terminal) are in front of 17 β -OH moiety and Trp741 (H6; N-terminal) and Met745 (H6) are over the steroid scaffold, whereas Gln711 (H3) is placed in front of the 3-keto carbonyl of testosterone. These conformational rearrangements may critically affect ligand accommodation into the binding site, so their side-chain flexibility was taken into account during docking simulations.

GOLD is more binding-site-dependent than other docking software. It has revealed well the exploration of conformational space and the generation of protein–ligand complexes, but it is significantly poorer when binding is predominantly driven by hydrophobic interactions,²⁰

as in the case of AR-LBP. Because of this, we used GOLD for geometrical definition and HINT for energetic evaluation of protein–ligand complexes generated by GOLD. Despite the enthalpic contribution to the free-energy calculation of protein–ligand interactions already considered by GOLD, the HINT scoring function allows the entropic contribution to the free-energy calculation associated with the displacement of water molecules from hydrophobic binding site by the ligand to be also taken into account. It is based on experimental Log $P_{o/w}$ values and includes the effects of solvation, enthalpic terms such as hydrogen bonding, Coulombic attractions, and hydrophobic attractions. The suitability of the algorithm was tested on a set of 53 protein–ligand complexes with and without water-molecule contributions.^{21,22} A linear regression was found between HINT score values and $\Delta G_{\text{binding}}$; the correlation between HS and $\Delta G_{\text{binding}}$ can be summarized by the following equation

$$\Delta G = -aH_{\text{TOT}} - b$$

where the values of a and b depend on the case study. As shown, H_{TOT} is inversely correlated to $\Delta G_{\text{binding}}$; negative ΔG values that are associated with a stable and energetically favored protein–ligand complex are identified by high HS values. In an example of virtual screening²³ where the model structures of 26 cyclin-dependent kinase inhibitor complexes were generated by docking (and thus not subject to crystallographic errors, etc.), HINT results were shown to correlate highly with inhibition. The regression of ΔG versus H_{TOT} for these data reflects the equation reported above with a SE of ± 0.3 kcal mol⁻¹ and r^2 of 0.94.

Therefore, to allow a proper evaluation of binding free energy in the case of the TX compounds, GOLD output was rescored with the HINT scoring function (hydrophobic interactions; <http://www.tripos.com/>). High HS (best interaction) are associated with low-free-energy levels for protein–ligand complexes.^{24,25} The HINT model describes specific atom–atom interactions between two molecules using the equation

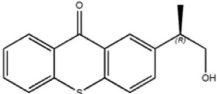
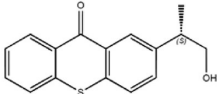
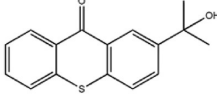
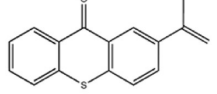
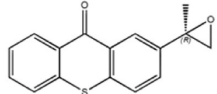
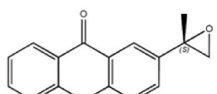
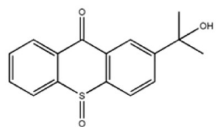
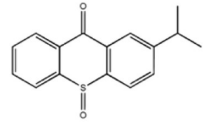
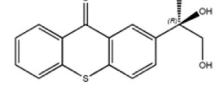
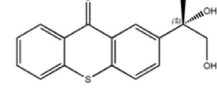
$$H_{\text{TOT}} = \sum \sum b_{ij} = \sum \sum (a_i s_i a_j s_j R_{ij} T_{ij} + r_{ij})$$

where a is the hydrophobic atom constant (derived from Log $P_{o/w}$), S is the solvent-accessible surface area, T is a function that differentiates polar–polar interactions (acid–acid, acid–base, or base–base), and R and r are functions of the distance between atoms i and j .²⁶ Each specific intra- and intermolecular atom(i)–atom(j) interaction is defined as the interaction score, b_{ij} , and gives an additive contribution to the global HINT score of protein–ligand association.

RESULTS AND DISCUSSION

As for other 3-keto nuclear receptors, the AR-LBD is configured as a hydrophobic site of accommodation for steroid ligands. As reported in Tables 3 and 4, HS values calculated for metabolites (**M1–M10** = experimental but also predicted *in silico*; **M11–M23** = only predicted *in silico*) are in close agreement with CoMSIA studies on steroidal and nonsteroidal chemicals as AR ligands by Wang and co-workers.²⁷ If the key phenomena for a good binding affinity of steroid derivatives are electrostatic (especially H-bonds), then the driving force of the binding process for nonsteroidal ligands is mainly hydrophobic. In Figure 5, comparisons between the binding orientations for endogenous AR ligand testosterone (**A**), one synthetic (2-ITX; **B1–2**), and one metabolic **M3**; **C1–2**) candidate are reported. The AR–testosterone binary complex is stabilized by hydrophobic interactions with the steroid scaffold. 17 β -OH in ring D acts as a H-bond donor for Asn705(H3) and as a H-bond acceptor for Thr877(H11), whereas the carbonyl oxygen in position 3 of ring A acts as a H-bond acceptor for the guanidine group of Arg752. Because of their planar structure, the binding poses for the TX compounds and testosterone are very closely related. A suitable occupation of the AR cavity is also observed

Table 3. Computational Prediction of Androgen-Mediated Endocrine-Disrupting Effects for Experimental Metabolites

COMPOUND	ABBREVIATION	STRUCTURE	HS	AFFINITY RATIO (HSComp/HSRef ^a)
(R)-2-(1-hydroxypropan-2-yl)-TX ⁷	M1		383	1.09
(S)-2-(1-hydroxypropan-2-yl)-TX ⁷	M2		373	1.07
2-(2-hydroxypropan-2-yl)-TX ⁷	M3		404	1.15
2-(prop-1-en-2-yl)-TX ⁷	M4		866	2.47
(R)-2-(2-methyloxiran-2-yl)-TX ⁷	M5		669	1.91
(S)-2-(2-methyloxiran-2-yl)-TX ⁷	M6		579	1.65
2-(2-hydroxypropan-2-yl)-TX-10-oxide ⁷	M7		155	0.44
2-isopropyl-TX-10-oxide ⁷	M8		176	0.50
(R)-2-(1,2-dihydroxypropan-2-yl)-TX ⁷	M9		Negative	-
(S)-2-(1,2-dihydroxypropan-2-yl)-TX ⁷	M10		126	0.36

^aReference compound, testosterone (HS = 350 pt). The affinity ratio is expressed as HS_{Comp}/HS_{ref}. The affinity ratio for testosterone is 1.

by docking simulations. **M7**, **M8**, **M9**, and **M10** are expected to be less capable of competing with testosterone for a stable accommodation into the binding site. In the case of the two 10-oxide derivatives, it could be due to steric and electronic clashes generated by the sulfoxide placed in front of Val746(H6),

Met787(H8), and Leu873(H11). It is interesting to note that the 1,2-diol moiety in **M9** and **M10** and the ternary alcohol in **M1** and **M2**, which differ only by an accessory hydroxyl functional group placed in C1', gives a significant lowering of the affinity.

Table 4. Computational Prediction of Androgen-Mediated Endocrine-Disrupting Effects for MetaPrint2D-React Metabolites

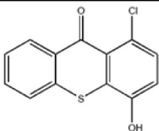
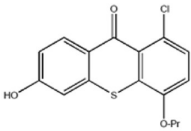
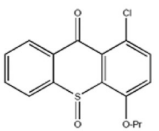
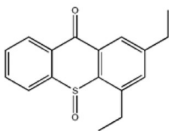
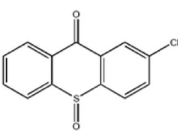
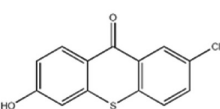
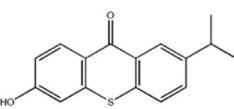
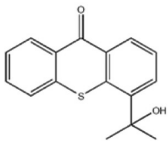
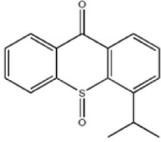
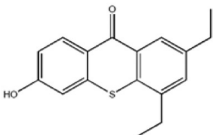
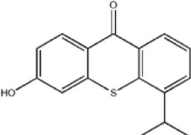
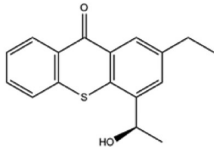
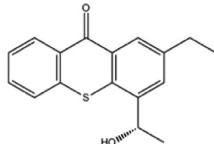
COMPOUND	ABBREVIATION	STRUCTURE	HS	AFFINITY RATIO (HSComp/HSRef ^a)
1-chloro-4-hydroxy-TX	M11		493	1.41
1-chloro-6-hydroxy-4-propoxy-TX	M12		453	1.29
1-chloro-4-propoxy-TX 10-oxide	M13		No Likely Pose	-
2,4-diethyl-TX 10-oxide	M14		341	0.97
2-chloro-TX-10-oxide	M15		88	0.25
2-chloro-6-hydroxy-TX	M16		1045	2.99
6-hydroxy-2-isopropyl-TX	M17		1138	3.25
4-(2-hydroxypropan-2-yl)-TX	M18		No Likely Pose	-
4-isopropyl-TX 10-oxide	M19		No Likely Pose	-

Table 4. continued

COMPOUND	ABBREVIATION	STRUCTURE	HS	AFFINITY RATIO (HSComp/HSRef ^a)
2,4-diethyl-6-hydroxy-TX	M20		879	2.71
6-hydroxy-4-isopropyl-TX	M21		1008	2.88
2-ethyl-4-((R)-1-hydroxyethyl)-TX	M22		125	0.36
2-ethyl-4-((S)-1-hydroxyethyl)-TX	M23		Negative	-

^aReference compound, testosterone (HS = 350 pt). The affinity ratio is expressed as HS_{Comp}/HS_{Ref}. The affinity ratio for testosterone is 1.

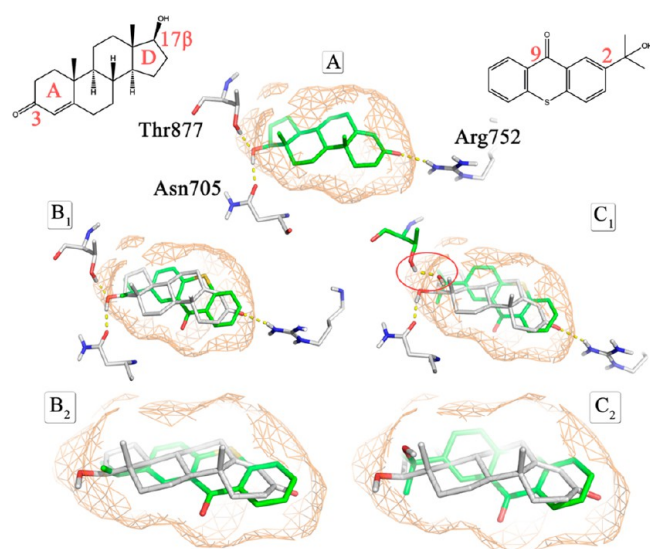


Figure 5. Comparison of binding models for natural ligand testosterone (T; A), 2-ITX (B1–2), and M3 (C1–2). (A) 17 β -OH edge of testosterone acts as a H-bond donor for Asn705(H3) and as a H-bond acceptor for Thr877(H11), whereas the C3=O edge acts as a H-bond acceptor for the guanidine group of Arg752. Both 2-ITX and M3 mimic the binding orientation of testosterone, giving a suitable occupation of the active site. The cavity shape is shown as a wheat wireframe.

In Figure 6, the predicted binding models for M9 (A), M1 (B), M7 (D), and M3 (E) are reported. The C1'–OH and C2'–OH of M9 act as a H-bond acceptor and H-bond donor for Thr877(H11) and Asn705(H3), respectively (Figure 6A). M1 gives only one H-bond with Thr877 (Figure 6B). A comparison between the 1,2-diol (in orange) and primary

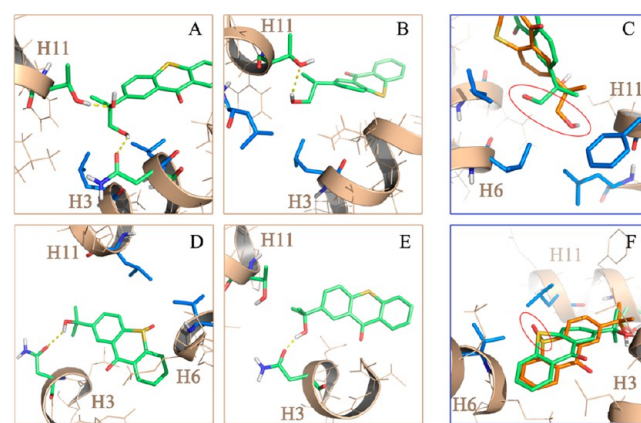


Figure 6. Graphic representation of the predicted binding poses for M9 (A), M1 (B), M7 (D), and M3 (E). Analysis of the negative effects generated by α -oriented hydroxyl groups (C) for 1,2-diol (in orange) and 2-hydroxyl derivatives and by the 10-sulfoxide moiety (in orange; F). Side chains that give negative ligand–receptor interactions are highlighted in blue sticks.

alcohol (in lime) (Figure 6C) reveals how the presence of polar groups lying in the N-terminal hydrophobic region of H11 can negatively affect binding affinity: the red-circled hydroxyl groups are in front of the Phe876, Leu873, Leu880 (H11), and Val746 (H6) hydrophobic side chains. Indeed, as demonstrated by Fang and co-workers²⁸ and Hong and co-workers,²⁹ the 17 β -OH configuration (over the steroid plane) of testosterone is important for binding affinity. α -Epitestosterone (OH lies under the steroid plane) shows a relative binding affinity (RBA) three times lower than the 17 β diastereoisomer. The tertiary alcohol of M7 (in orange) and M3 (in lime) act as a H-bond donor for Asn705 (H3) (Figure 6D,E). A comparison between these two compounds (Figure 6F) reveals how the red-circled sulfoxide is poorly tolerated by the binding pocket: it lies in front of the hydrophobic side chains of Leu873 (H11) and Val746 (H6), giving negative hydrophobic/polar interactions. No likely pose was reached for M13, M18, and M19 because of electronic and steric clashes generated by the sulfoxide and hydroxyl groups in C4. HINT scores under the cutoff and affinity ratios less than 1 are predicted for M15, M22, M14, and M23. A C6-hydroxyl group is revealed as being good at promoting ligand–receptor interaction. With the exception of M12, affinity ratios greater than 2 were obtained for M17, M21, M20, and M16. The bulky C4-propoxy group significantly affects HS values for M12, giving an affinity ratio of 1.29. The C6-hydroxyl group H-bonds with Gln711(H3), Met745(H6), and Arg752(H6) (data not shown).

Briefly, the *in silico* results can be summarized as follows: a 10-oxide group is poorly tolerated, whereas a 2-(1,2-dihydroxypropan-2-yl) substituent gives steric and electronic clashes that reduce binding affinity. Except for M7, M8, M9, M10, M14, M15, and M22 and those that were negative controls, the affinity ratios for all of the tested compounds go from 1 to 3.5, showing that these compounds could act as competitors of testosterone for the steroid-binding site.

CONCLUSIONS

The case study of TX compounds and their metabolites is an application of a more general computational approach to some phases of toxicokinetic/toxicodynamic studies. We are conscious of the small size of the validation set, but no other data are currently available. Additionally, these data have allowed us to generate a good local model to study the thioxanthone scaffold and were able to predict correctly the experimental results. A dimensionally restricted and chemically homogeneous validation set can allow for the building of accurate, simple, and plastic local models for efficient preliminary filtering. The approach is not intended as a stand-alone protocol but rather as a valid and innovative support for use in the preliminary stages of safety assessment.

Because no toxicological data on TX metabolites is available, our results suggest that hazard evaluation could be necessary to avoid a potential underestimation of the toxicological risk for this class of chemicals.

AUTHOR INFORMATION

Corresponding Author

*E-mail pietrocozzini@unipr.it; Phone: +39 0521 905669; Fax: +39 0521 905556.

Notes

The authors declare no competing financial interest.

ACKNOWLEDGMENTS

We thank Dr. M. Reitsma of the RIKILT-Institute of Food Safety, Wageningen UR, Wageningen and Dr. S. Aprile of the Dipartimento di Scienze Chimiche, Alimentari, Farmaceutiche e Farmacologiche and Drug and Food Biotechnology Center, Università degli Studi del Piemonte Orientale A. Avogadro for the scientific material that they kindly provided. We also thank Prof. Glen E. Kellogg, Department of Medicinal Chemistry, Virginia Commonwealth University, for the use of the HINT software.

ABBREVIATIONS

AhR, aryl hydrocarbon receptor; AR-LBP, androgen receptor ligand binding pocket; CoMSIA, comparative molecular similarity index analysis; CTD, C-terminal domain; DHT, dihydrotestosterone; DR CALUX, dioxin receptor chemical activated luciferase gene expression assay; EHDAB, 2-ethylhexyl-4-dimethylaminobenzoate; GA, genetic algorithm; HINT, hydrophobic interaction; HLM, human liver microsomes; HS, HINT Score; ITX, isopropylthioxanthone; LC/MS, liquid chromatography/mass spectrometry; LC/UV, liquid chromatography/ultraviolet; RBA, relative binding affinity; RLM, male Wistar rat liver microsomes; SOM, site of metabolism

REFERENCES

- (1) EFSA (European Food Safety Authority) (2005) Opinion of the scientific panel of food additives, flavourings, processing aids and materials in contact with food on a request from the commission related to 2-isopropylthioxanthone (ITX) and 2-ethylhexyl-4-dimethylaminobenzoate (EHDAB) in food contact materials. *EFSA J.* 293, 1–15.
- (2) Peijnenburg, A., Riethof-Poortman, J., Baykus, H., Portier, L., Bovee, T., and Hoogenboom, R. (2010) AhR-agonistic, anti-androgenic, and anti-estrogenic potencies of 2-isopropylthioxanthone (ITX) as determined by *in vitro* bioassays and gene expression profiling. *Toxicol. In Vitro* 24, 1619–1628.
- (3) Reitsma, M., Bovee, T. F., Peijnenburg, A. A., Hendriksen, P. J., Hoogenboom, R. L., and Rijk, J. C. (2013) Endocrine-disrupting effects of thioxanthone photoinitiators. *Toxicol. Sci.* 132, 64–74.
- (4) Germain, P., Staels, B., Dacquet, C., Spedding, M., and Laudet, V. (2006) Overview of nomenclature of nuclear receptors. *Pharmacol. Rev.* 58, 685–704.
- (5) Claessens, F., Verrijdt, G., Schoenmakers, E., Haelens, A., Peeters, B., Verhoeven, G., and Rombauts, W. (2001) Selective DNA binding by the androgen receptor as a mechanism for hormone-specific gene regulation. *J. Steroid Biochem. Mol. Biol.* 76, 23–30.
- (6) Li, J., and Al-Azzawi, F. (2009) Mechanism of androgen receptor action. *Maturitas* 63, 142–148.
- (7) Aprile, S., Del Grosso, E., and Groso, G. (2011) *In vitro* metabolism study of 2-isopropyl-9H-thioxanthene-9-one (2-ITX) in rat and human: evidence for the formation of an epoxide metabolite. *Xenobiotica* 41, 212–225.
- (8) Pereira de Jésus-Tran, K., Côté, P. L., Cantin, L., Blanchet, J., Labrie, F., and Breton, R. (2006) Comparison of crystal structures of human androgen receptor ligand-binding domain complexed with various agonists reveals molecular determinants responsible for binding affinity. *Protein Sci.* 15, 987–999.
- (9) Bovee, T. F. H., Helsdingen, J. R., Rietjens, I. M. C. M., Keijer, J., and Hoogenboom, L. A. P. (2004) Rapid yeast estrogen bioassays stably expressing human estrogen receptors α and β , and green fluorescent protein: A comparison of different compounds with both receptor types. *J. Steroid Biochem. Mol. Biol.* 91, 99–109.
- (10) Bovee, T. F. H., Helsdingen, J. R., Hamers, A. R. M., Duursen, M. B. M., Nielen, M. W. F., and Hoogenboom, L. A. P. (2007) A new highly specific and robust yeast androgen bioassay for the detection of agonist and antagonists. *Anal. Bioanal. Chem.* 389, 1549–1558.

- (11) McLean, M. R., Bauer, U., Amaro, A. R., and Robertson, L. W. (1996) Identification of catechol and hydroquinone metabolites of 4-monochlorobiphenyl. *Chem. Res. Toxicol.* 9, 158–164.
- (12) Amaro, A. R., Oakley, G. G., Bauer, U., Spielmann, H. P., and Robertson, L. W. (1996) Metabolic activation of PCBs to quinones: Reactivity toward nitrogen and sulfur nucleophiles and influence of superoxide dismutase. *Chem. Res. Toxicol.* 9, 623–629.
- (13) Lehmler, H. J., and Robertson, L. W. (2001) Synthesis of hydroxylated PCB metabolites with the Suzuki-coupling. *Chemosphere* 45, 1119–1127.
- (14) Boyer, S., Arnby, C. H., Carlsson, L., Smith, J., Stein, V., and Glen, R. C. (2007) Reaction site mapping of xenobiotic biotransformations. *J. Chem. Inf. Model.* 47, 583–590.
- (15) Carlsson, L., Spjuth, O., Adams, S., Glen, R. C., and Boyer, S. (2010) Use of historic metabolic biotransformation data as a means of anticipating metabolic sites using MetaPrint2D and Bioclipse. *BMC Bioinf.* 11, 362.
- (16) Jones, G., Willett, P., and Glen, R. C. (1995) A genetic algorithm for flexible molecular overlay and pharmacophore elucidation. *J. Comput.-Aided Mol. Des.* 9, 532–549.
- (17) Jones, G., Willett, P., Glen, R. C., Leach, A. R., and Taylor, R. (1997) Development and validation of a genetic algorithm for flexible docking. *J. Mol. Biol.* 267, 727–748.
- (18) Duke, C. B., Jones, A., Bohl, C. E., Dalton, J. T., and Miller, D. D. (2011) Unexpected binding orientation of bulky-B-ring anti-androgens and implications for future drug targets. *J. Med. Chem.* 54, 3973–3976.
- (19) Cantin, L., Faucher, F., Couture, J. F., de Jésus-Tran, K. P., Legrand, P., Ciobanu, L. C., Fréchette, Y., Labrecque, R., Singh, S. M., Labrie, F., and Breton, R. (2007) Structural characterization of the human androgen receptor ligand-binding domain complexed with EM5744, a rationally designed steroidal ligand bearing a bulky chain directed toward helix 12. *J. Biol. Chem.* 282, 30910–30919.
- (20) Perola, E., Walters, W. P., and Charifson, P. S. (2004) A detailed comparison of current docking and scoring methods on systems of pharmaceutical relevance. *Proteins* 56, 235–249.
- (21) Cozzini, P., Fornabaio, M., Marabotti, A., Abraham, D. J., Kellogg, G. E., and Mozzarelli, A. (2002) Simple, intuitive calculations of free energy of binding for protein-ligand complexes. 1. Models without explicit constrained water. *J. Med. Chem.* 45, 2469–2483.
- (22) Fornabaio, M., Cozzini, P., Mozzarelli, A., Abraham, D. J., and Kellogg, G. E. (2003) Simple, intuitive calculations of free energy of binding for protein-ligand complexes. 2. Computational titration and pH effects in molecular models of neuraminidase-inhibitor complexes. *J. Med. Chem.* 46, 4487–4500.
- (23) Gussio, R., Zaharevitz, D. W., McGrath, C. F., Pattabiraman, N., Kellogg, G. E., Schultz, C., Link, A., Kunick, C., Leost, M., Meijer, L., and Sausville, E. A. (2000) Structure-based design modifications of the paullone molecular scaffold for cyclin-dependent kinase inhibition. *Anti-Cancer Drug Des.* 15, 53–66.
- (24) Fornabaio, M., Spyraakis, F., Mozzarelli, A., Cozzini, P., Abraham, D. J., and Kellogg, G. E. (2004) Simple, intuitive calculations of free energy of binding for protein-ligand complexes. 3. The free energy contribution of structural water molecules in HIV-1 protease complexes. *J. Med. Chem.* 47, 4507–4516.
- (25) Marabotti, A., Spyraakis, F., Facchiano, A., Cozzini, P., Alberti, S., Kellogg, G. E., and Mozzarelli, A. (2008) Energy-based prediction of amino acid-nucleotide base recognition. *J. Comput. Chem.* 29, 1955–1969.
- (26) Kellogg, G. E., and Abraham, D. J. (2000) Hydrophobicity: Is LogP(o/w) more than the sum of its parts? *Eur. J. Med. Chem.* 35, 651–661.
- (27) Wang, X., Li, X., Shi, W., Wei, S., Giesy, J. P., Yu, H., and Wang, Y. (2012) Docking and CoMSIA studies on steroids and non-steroidal chemicals as androgen receptor ligands. *Ecotoxicol. Environ. Saf.* 89, 143–149.
- (28) Fang, H., Tong, W., Branham, W. S., Moland, C. L., Dial, S. L., Hong, H., Xie, Q., Perkins, R., Owens, W., and Sheehan, D. M. (2003) Study of 202 natural, synthetic, and environmental chemicals for binding to the androgen receptor. *Chem. Res. Toxicol.* 16, 1338–1358.
- (29) Hong, H., Fang, H., Xie, Q., Perkins, R., Sheehan, D. M., Tong, W. Comparative molecular field analysis (CoMFA) model using a large diverse set of natural, synthetic and environmental chemicals for binding to the androgen receptor. *SAR QSAR Environ. Res.* 14, 373–388.